Starburst Polyelectrolytes: Scaling and Self-Consistent-Field Theory

J. Klein Wolterink,[†] J. van Male,[†] M. Daoud,[‡] and O. V. Borisov*[,§,⊥]

Wageningen University, Laboratory for Physical Chemistry, and Colloid Science, 6703 HB Wageningen, The Netherlands; Service de Physique de l'Etat Condensé, CE-Saclay, 91191 Gif sur Yvette, France; Institute of Macromolecular Compounds of the Russian Academy of Sciences, 199004, St. Petersburg, Russia; and LRMP/UMR 5067, Helioparc Pau-Pyrenees, 64053 Pau, France

Received March 26, 2003; Revised Manuscript Received June 4, 2003

ABSTRACT: Conformations of weakly charged starburst polyelectrolytes in dilute solution are studied as a function of the number of generations *g*, the length of spacers *n*, and the degree of ionization α. Scaling analysis is combined with extensive numerical self-consistent-field (SCF) calculations performed on the basis of an extended Scheutjens−Fleer (SF) algorithm. We demonstrate that the predictions of scaling analysis are applicable only for starburst polyelectrolytes with relatively small number of generations and sufficiently long spacers. We prove that irrespective of the strength/type of the intramolecular interactions the starburst macromolecules are characterized by a monotonic decay of the density profiles in the radial direction. In the case of a large number of generations a quasi-plateau in the monomer density profile is observed. This leveled-off distribution of density is due to strong fluctuations in the radial positions of branching points and end segments. In accordance with earlier Monte Carlo simulations results, we observe that the outer generations pull strongly on the spacers of inner generations.

1. Introduction

Starburst polymers (or flexible chain dendrimers) present an important class of regularly branched polymers. The structural properties and interactions of nonionic dendrimers were extensively studied both theoretically[1−3] and experimentally.[4−8]

Recently, charged (ionic) starburst polymers have attracted considerable attention due to their potential biomedical applications (e.g., in drug delivery systems, gene therapy, etc.). From this perspective, the still unresolved question concerning internal structure of the dendrimers has a major importance for their absorbing (or trapping) "capacity". In the earlier theory of de Gennes and Hervet,[1] a monotonical increase in the intramolecular density as a function of distance from the center ("hollow dendrimer") was predicted. However, neither experiments[9,10] nor computer simulations[3,11−16] support this picture. Even more intriguing is this question about the internal structure for charged starburst macromolecules (or dendrimers), where strong intramolecular Coulomb interactions lead to strong extension of the spacers belonging to earlier generations.

The neutron and X-ray scattering experiments provide information about both the internal structural organization (e.g., radial polymer density distribution) and the interaction between dendrimers in solution[4−9] via the *q* dependences of the form factor and structure factors, respectively. All the available experimental data indicate compact (fairly homogeneous) internal structure of dendrimers and "soft" repulsive interaction between the dendrimers in solution. (The structure factors can be well-fitted on the basis of Yukawa interaction potential.) In most cases, however, nonionic dendrimers with comparatively short spacers and therefore a limited number of generations (usually up to 5) were studied.

There is an important difference in the behavior of neutral and charged (ionic) branched polymers. In the former case extension of branches is due to short-range steric (excluded volume) interactions between monomers of the branches. In the latter case the main contribution to the intramolecular repulsion is due to Coulomb interaction between charged monomers or due to a high osmotic pressure within the branched molecule. This high osmotic pressure is created by the accumulations of small mobile ions which are preferentially localized near the charged molecule, even if no salt is added (charge renormalization).

It has been well established that the charge renormalization effect (localization of counterions), as first described by Alexander et al.[17] for charged colloids, is an inherent property of strongly (regularly as well as randomly) branched polyelectrolytes.[18−22] Because of the connectivity of charged monomers in the branched macroion, the charges of the macroion are localized in a relatively small intramolecular volume and create a strong attractive Coulombic potential for mobile counterions. In salt-free solution, this Coulomb attraction overcomes the gain in translational entropy upon uniform distribution of the counterions in a large (though finite) volume of the solution. The onset of the charge renormalization corresponds to characteristic degree of branching, which depends on the fraction of charged monomers.

The aim of the present paper is to analyze theoretically the equilibrium conformational structure of flexible-chain ionic dendrimes (starburst polyelectrolytes) in dilute solutions. Hence, we are not going to address the problem of "soft" interactions between the ionic dendrimers. (A theoretical analysis of interaction between star-branched polyelectrolytes in solutions can be found in ref 21.)

We are going to focus on the effects of the molecular architectural parameters, e.g., the number of generations *g* and the length of spacer chains *n*, and of the intramolecular interactions (tunable electrostatic vs steric repulsions) on the internal conformational struc-

[†] Wageningen University.
[‡] Service de Physique de l'Etat Condensé.
[§] Russian Academy of Sciences.
[⊥] LRMP/UMR 5067.

10.1021/ma030187p CCC: $25.00
Published on Web 07/24/2003

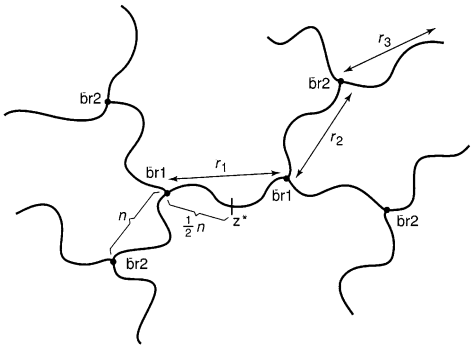

Figure 1. Starburst polyelectrolyte with two generations.

ture of the starburst polyelectrolytes. The radial dependence of the intrachain tension and the fluctuational behavior of the branches are of particular interest of us, as they appear to be essentially different from those found for other types of branched and grafted polymer architectures. We aim to combine two types of theoretical approaches, i.e., (i) the Flory-type analysis which enables us to obtain the power-law dependencies of the overall size of the starburst polyelectrolyte on the main parameters and (ii) the numerical self-consistent-field calculations, which give an important insight into the internal structure and fluctuations in starburst polyelectrolytes. The latter approach enables to obtain structural properties of the macromolecular systems with the accuracy close to that available in Monte Carlo simulations,[12] but with much higher efficiency. As a result, we are able to analyze structure of flexible chain ionic dendrimers with long spacers and large number of generations.

The rest of the paper is organized as follows. In section 2 we describe the model of a charged starburst polymer. In section 3 the analytical Flory-type approach is presented. The numerical procedure is described in section 4. This is followed by the results in section 5. In section 6 we summarize our results and conclusions.

2. Model

We consider the starburst polymer of $g \geq 0$ generation (see Figure 1). We assume that each branching point has a functionality 2, i.e., three spacers, one spacer of the generation j and two spacers of the generation $j + 1$ join in a branching point. Each spacer is a linear polymer chain comprising n monomers. The total number of monomers in the polymer N is

$$N(g) = n(2^{g+1} - 3) \cong 2^{g+1}n, \quad g = 1, 2, ... \qquad (1)$$

and the last equality is valid for $g \gg 1$.

The spacers are assumed to be intrinsically flexible (the statistical segment length is of the order of a monomer unit length a, which is taken as the unit length in our subsequent analysis) and weakly charged, i.e., comprise the fraction $\alpha \ll (a/l_B)^2 \cong 1$ of charged monomers. Here $l_B = e^2/k_BT\epsilon$ is the Bjerrum length, which is of order 0.7 nm in water under normal conditions (e is the elementary charge, ϵ is the dielectric constant of the solvent, T is the temperature, and k_B is the Boltzmann constant). The fraction of charged monomers α is assumed to be quenched, i.e., independent of the external conditions and chain extension. Because of the electroneutrality condition, the solution contains small mobile counterions which compensate the overall charge αN of the macroion and, in general case, also salt. All mobile ions are assumed to be monovalent. The salt concentration, c_s, in the bulk of the solution determines the Debye screening length, $\kappa^{-1} \cong (l_B c_s)^{-1/2}$. We assume that the solution of starburst macroions is dilute, and any intermolecular interactions can be safely neglected.

The nonelectrostatic, short-range interactions between uncharged monomer units are described by the dimensionless second, v, and the third, $w \sim 1$, virial coefficients which are normalized by the factors a^{-3} and a^{-6}, respectively.

3. Flory Theory

We start with developing a Flory-type argument for establishing a relation between the dimensions of the starburst polyelectrolytes and their molecular parameters. Our approach is similar to (though slightly different from) that suggested earlier by Boris and Rubinstein[2] for neutral starbursts. (In particular, in contrast to refs 2 and 12, our approach assumes an explicit counting of the conformational entropy losses in all the extended spacers.) The electrostatic interactions are incorporated using the same approach as earlier for star-branched[19,20] polyelectrolytes. The latter enables to obtain proper crossover between low and high salt regimes.

The application of the mean-field Flory-type approach assumes minimization of the free energy of the starburst macromolecule. The free energy comprises the entropic term, F_{conf} (describing the conformational entropy penalty for the extension of all the spacers), and the interaction term, F_{int}, which accounts for repulsive intramolecular interaction within the starburst polymer

$$F = F_{conf} + F_{int} \qquad (2)$$

If Δr_i is the (average) radial extension of spacers of generation i, then the total conformational free energy of the polymer can be obtained by summation over all the generations as

$$F_{conf}/k_BT \cong \frac{3}{2}\left(\frac{\Delta r_1^{\,2}}{n} + \sum_{j=2}^{g} 2^j \frac{\Delta r_j^{\,2}}{n}\right) \qquad (3)$$

where $3\Delta r_j^2/2n$ is the elastic free energy stored in each extended spacer of generation j. Here we assume uniform distribution of the local tension within each spacer. Using the condition of the elastic force balance in each branching point, $\Delta r_j \cong 2\Delta r_{j+1}$, we find that the average radial extension of the spacer decays exponentially as a function of the ranking number of the generation

$$\Delta r_j \cong \Delta r_1/2^{j-1}, \quad j = 1, 2, ..., g \qquad (4)$$

and the total radius of the starburst polymer can be written as

$$R(g) \cong \Delta r_1/2 + \sum_{j=2}^{g} \Delta r_j \cong \frac{3}{2}\Delta r_1\left(1 - \frac{4}{3}2^{-g}\right) \qquad (5)$$

Using eqs 3 and 5, we find that

$$F_{conf}/k_BT \cong \frac{2R^2(g)}{n}\left(1 - \frac{4}{3}2^{-g}\right)^{-1} \qquad (6)$$

In the case of neutral starbursts the elastic free energy, eq 6, has to be balanced with the free energy of the short-range steric repulsion between the monomers. Following the classical Flory approach, the latter contribution can be written in a virial approximation as

$$F_{\text{int}} \cong \begin{cases} vN^2(g)/R^3(g), & \text{good solvent} \\ wN^3(g)/R^6(g), & \Theta \text{ solvent} \end{cases} \quad (7)$$

Two important features of eq 7 are as follows: (i) We effectively smear out the monomer density over the volume occupied by the starburst polymer, i.e., we assume fairly uniform density distribution; this is well-justified by the results of numerical calculations presented below. (ii) We neglect contributions of higher order interactions, e.g., ternary interactions in the good solvent regime; this approximation is definitely violated for starbursts with sufficiently short spacers and sufficiently high number of generations (leading to high intramolecular density).

Upon minimization of the free energy given by eqs 2, 6, and 7, we find

$$R(g) \cong \begin{cases} N^{2/5}(g)v^{1/5}n^{1/5} & \text{good solvent} \\ N^{3/8}(g)n^{1/8} & \Theta \text{ solvent} \end{cases} \quad (8)$$

Two observations in eq 8 can be made: (i) for $g \cong 1$, $N(g) \cong n$ and the scaling exponents typical for linear chains in good or Θ-solvent ($R \sim N^{3/5}$ or $R \sim N^{1/2}$, respectively) are obviously recovered; (ii) the exponents are different from those obtained by Boris and Rubinstein[2] due to different counting of the conformational entropy in our case.

Remarkably, the scaling behavior $R(g) \sim N^{2/5}(g)$ and $R(g) \sim N^{3/8}(g)$ for good or Θ conditions, respectively, follows from the very general arguments: the number of monomers in a starburst polymer grows exponentially with g, while the size of an ideal (without intramolecular interactions) starburst grows as $\sim g^{1/2}$, just as for a linear Gaussian chain. Hence, the Flory exponent ν for the size of an ideal starburst ($R \sim N^{\nu}$) is equal to zero. As $F_{\text{conf}} \sim R^2(g)/R^2_{\text{ideal}}(g)$ we recover the result of eq 8.

For the analysis of the conformations of a charged starburst, it is more convenient to start from the case, when the intramolecular Coulomb interactions between monomers are partially screened by the mobile ions of added low molecular weight salt. It is well-known (see e.g. refs 20 and 22) that in this regime the repulsive Coulomb interactions inside branched polyelectrolyte can be described as short-range binary repulsion with the effective second virial coefficient $v_{\text{eff}} \cong l_B\kappa^{-2} \cong \alpha^2/c_s$. (The latter expression for the second virial coefficient of interaction between charged particles can be obtained by direct calculation using Debye−Huckel screened electrostatic potential.) Hence, eq 8 with v substituted by v_{eff} can be used. Correspondingly, the dimensions of the starburst polyelectrolyte in the salt-dominance regime are expected to scale as

$$R(g) \cong N^{2/5}(g)\alpha^{2/5}n^{1/5}c_s^{-1/5} \quad (9)$$

i.e., the size of the starburst polymer decays as $\sim c_s^{-1/5}$ with increasing salt concentration due to enhanced screening, similar to the case of starlike polyelectrolytes.[20]

Equation 9 is valid at sufficiently high salt concentration, when screening of the Coulomb interaction inside the starburst polyion is ensured by mobile ions of added salt. On the contrary, if no salt is added, the intramolecular screening is ensured predominantly by counterions trapped in the intramolecular volume of the starburst polyelectrolyte. This regime is also referred to as an "osmotic" regime because swelling of the branched polyelectrolyte is ensured by osmotic pressure of counterions trapped in the intramolecular space of the branched polyion. In the general case, the osmotic regime occurs for sufficiently strongly branched polyions in a salt-free solution. The crossover between the salt-dominated regime and the osmotic regime occurs when the concentration of added salt c_s is roughly equal to the intramolecular concentration of trapped counterions $c^* \sim \alpha N(g)/R^3(g)$.

The power law dependence for the dimensions of the branched polyion in the osmotic regime can be derived from the conditions of the crossover at $c_s \cong c^*$. Equivalently, one can apply eq 9 with c_s substituted by c^*. As a result, we obtain for the starburst polyelectrolyte swollen in the osmotic regime

$$R(g) \cong N^{1/2}(g)\alpha^{1/2}n^{1/2} \quad (10)$$

and the crossover between the osmotic and the salt-dominated regimes occurs at

$$c_s \cong c^* \cong (\alpha N(g))^{-1/2}n^{-3/2} \quad (11)$$

Remarkably, the $R(g) \sim \alpha^{1/2}$ dependence, typical in the osmotic regime for all types of branched polyions with Gaussian elasticity of branches, is found.

There is, however, an important difference between eq 10 and the analogous ones for star-branched polyelectrolytes or polyelectrolyte brushes.[18,23,24]

In the latter two systems the local tension in the polyelectrolyte chains scales proportionally to $\alpha^{1/2}$ and is independent of the number of branches in a star or of the grafting density in the brush (and independent of the chain length). As a consequence, the thickness of the brush or the size of the star in the osmotic regime is independent of the number of linear chains involved, i.e., of the degree of branching. A similar situation occurs in randomly branched polyelectrolytes.[22]

If the same arguments could be applied for a starburst polyelectrolyte, then the size in the osmotic regime would be given by $R(g) \cong \alpha^{1/2}ng$, where ng is simply the number of monomers in the chemical path from the center of the starburst to the free end segments of the outermost generation and the presence of other (side) branches would be irrelevant. The difference between this result and that presented in eq 10 is due to the fact that in the case of a starburst polyelectrolyte local extension of the spacers of inner generations is always stronger than that of outer generations, and therefore, the size of the starburst polyelectrolyte in the osmotic regime depends on the total number of branches and not only on the number ng of monomers in the chemical path from the center to the end segments.

The effect of charged renormalization (localization of counterions inside the branched polyelectrolyte) occurs only for sufficiently strongly branched polyions, whose bare charge is sufficiently high and is localized in sufficiently small volume. This enables to overcome the translational entropy and to retain mobile counterions in the intra-macromolecular space. The onset of charge

renormalization (the other boundary of the osmotic regime) corresponds to the condition $\alpha N(g) \geq R(g)/l_B$ that is

$$(N(g^*)/n) \geq (\alpha^{1/2} l_B)^{-2} \quad (12)$$

Hence, the characteristic number of generations g^* above which counterions remain trapped inside the starburst polyelectrolyte, as given by eq 12, depends only on the coupling parameter $\alpha^{\nu} l_B$ and decreases with increasing $\alpha^{\nu} l_B$. (In our case $\nu = 1/2$, as long as Gaussian elasticity of spacers is assumed.) Remarkably, g^* is independent of the number of monomers per spacer n (since $N(g) \sim n$).

This behavior has its analogy for starlike or for randomly branched polyelectrolytes, where charge renormalization (osmotic behavior) occurs when the number of branches exceeds some characteristic values, which also scales as $(\alpha^{\nu} l_B)^m$. The power law exponent m depends on the particular topology of the branched polyion.[19,22]

Finally, for starburst polyelectrolytes with $g \leq g^*$ in a salt-free solution no charge renormalization and no intramolecular screening of the Coulomb interactions occur. The dimensions of the charged starburst polymer in this regime can be obtained by the setting $g \cong g^*$ in eq 10 or directly by balancing the elastic free energy, eq 6, and the energy of unscreened Coulomb repulsion $F_{Coulomb} \cong l_B \alpha^2 N(g)^2/R(g)$ that results in

$$R(g) \cong N^{2/3}(g) n^{1/3} (\alpha^2 l_B)^{1/3} \quad (13)$$

The main limitation of all the derived above equations for the size of a starburst polymer as a function of the number of generations g, degree of ionization α, and spacer length n is due to assumed above Gaussian elasticity of spacers (eqs 3 and 6). As our numerical calculations indicate, the extension of the spacers of earlier generations strongly increases with increasing total number of generations and reaches the limit of extensibility (the inner spacers are completely extended) even in the starbursts with relatively small number of generations. Therefore, for sufficiently large g eqs 8−10 and 13 systematically overestimate the size of a starburst polymer. This has to be kept in mind upon an analysis of the numerical results presented in the following sections.

4. Numerical SCF Model

The numerical SCF approach is based on the Scheutjens−Fleer (SF) algorithm. This algorithm was first proposed for neutral polymers at interfaces[25,26] and extended to account for electrostatics on a Poisson−Boltzmann level[27] and later generalized by Van Male et al.[28] for spherical geometry and for calculating chemical reactions. The extension for the calculations to branched polyelectrolytes has been performed in the past for SF-SCF calculations by Leermakers et al.[32] and Van der Linden et al.[31] All the calculations were done with the software package "sfbox".[29,30] Some information on the SF-SCF model is given below, especially a way to calculate the starbursts. For full details the reader should consult the literature references quoted above.

The SF-SCF approach uses a lattice which facilitates to account for the volume of all molecular components. A lattice cell with the size a of 0.6 nm ($\approx$ the Bjerrum length) can be occupied either by a solvent molecule S, a polymer segment P, or a mobile ion. We assume that there are two types of ions in the system: co-ions, Cl^-, and counterions, Na^+ (polymer segments are assumed to be negatively charged). The lattice cells are arranged in an array of concentric spherical shells (or "layers") numbered as $z = 1,..., M$; the outer surface of the zth layer is at the distance $r = za$ from the center. The total cell radius is given by $D = Ma$. The volume of the system within the shell number z is given by $V(z) = {}^4/_3\pi(za)^3$, and a layer at coordinate z contains $L(z) = (V(z) - V(z-1))/a^3 = 4\pi(z^2 - z + {}^1/_3)$ lattice "sites". The dimensionless inner area a_i and outer area a_o of a lattice site in layer z are given by $a_i(z) = 4\pi(z-1)^2/L(z)$ and $a_o(z) = 4\pi z^2/L(z)$, respectively. These quantities determine the so-called a priori step probabilities, $\lambda(z,z')$, for steps from layer z to z', where z' takes the values $z-1$ (to the inner layer), $z+1$ (to the outer layer), or z (within the same layer). The step probabilities are given by $\lambda(z, z-1) = a_i(z)/6$, $\lambda(z, z+1) = a_o(z)/6$, and $\lambda(z, z) = 1 - \lambda(z, z+1) - \lambda(z, z-1)$, respectively.

The SCF formalism features the particle potentials $u_x(z)$ which are conjugated to the volume fractions $\varphi_x(z)$. Subscript x is used to refer to the various types of particles x = S, P, Na^+, Cl^-. The functionals $u_x(z)$ and $\varphi_x(z)$ are mutually dependent and are, for a given particle type, only functions of the z coordinate. Hence, all the local properties of the system are preaveraged over the angular coordinates (the spherical approximation). The total potential of a particle of type x comprises three terms:

$$u_x(z) = u'(z) + k_B T \sum_y \chi_{xy}(\langle\varphi_y(z)\rangle - \varphi_y^b) + \nu_x e\psi(z) \quad (14)$$

The first term is coupled to the incompressibility constraint $\sum_x \varphi_x(z) = 1$. The second term gives the short-range interactions, parametrized by Flory−Huggins interaction parameters χ_{xy} between particle types x and y; this interaction term depends on the volume fraction of the components. The term $\langle\varphi_y(z)\rangle$ is the site average volume fraction, which is equal to $\lambda(z, z-1)\varphi_y(z-1) + \lambda(z, z)\varphi_y(z) + \lambda(z, z+1)\varphi_y(z+1)$ (note that the site fraction causes the potential to be nonlocal and geometry dependent). The quantity φ_y^b in eq 14 is the concentration of monomers of type y in the bulk. The third term accounts for the electrostatic contributions. The local charge $q(z)$ per lattice site is given by $q(z) = e\sum_x \nu_x \varphi_x(z)$, where e is the elementary charge and ν_x the valence of the particle of type x. The local electrostatic potential, $\psi(z)$, is related to the local charge density, $q(z)$, via the Poisson equation.

To obtain the density profiles $\varphi_x(z)$ from the segment potentials $u_x(z)$, one has to evaluate all possible and allowed conformations of the molecules in the potential field. In the special case of a dendrimer which is grafted by the middle segment, one has to consider the grafting constraint present on the first segments of each arm. In a first-order Markov approximation, one can compare the chain conformations of one arm of the star with segments $s = 1, ..., E$ with the path of a diffusing particle in an external field that starts in (or near) the center of the coordinate system and ends up somewhere in the system at a time t (=E). The corresponding diffusion equation features end-point distribution functions $G_P(z,s|z^*,1)$ for the statistical weight of finding a chain fragment that starts with segment $s = 1$ at z^* (grafting point) and ends in layer z with segment s, and correspondingly $G_P(z,s|E)$ for the statistical weights of

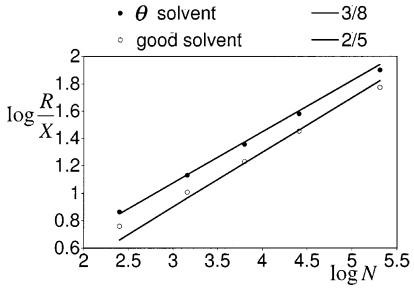

Figure 2. Size as a function of the total number of monomers N. The size is normalized as denoted in eq 8.

all possible and allowed conformations, with the specification that segment $s = E$ can be anywhere in the system and again segment s is at coordinate z. Hence, $G_P(z,s|E)$ is the sum of $G_P(z,s|z',E)$ over all z'. The endpoint distribution functions obey, as already mentioned, the diffusion equation which, in discrete notation, can be written as

$$G_p(z, s|z^*, 1) = G_p(z)\langle G_p(z,s-1|\, z^*, 1)\rangle$$
$$G_p(z,s|E) = G_p(z)\langle G_p(z,s+1|E)\rangle \qquad (15)$$

These propagator relations are started by the condition that a "walk" of one segment long should be weighted by the free segment distribution function: $G_P(z,E|E) = G_P(z)$ for all z and $G_P(z^*,1|z^*,1) = G_P(z^*)$ (grafting condition). The segmental weighting factor $G_P(z)$ is defined as $\exp(-u_P(z)/k_BT)$. The segment densities follow from the composition law:

$$\varphi_p(z,s) = C_p \frac{G_p(z,s|z^*,1)G_p(z,s|E)}{G_p(z)} \qquad (16)$$

Here, the factor $G_P(z)$ in the denominator corrects for the double counting of the Boltzmann weight for segment s in the nominator. The normalization factor C_P is fixed by the number $N(s)$ of monomers of the monomer with ranking number s:

$$C_p = N(s) \qquad (17)$$

The grafting coordinate of the middle segment of the arms is the first shell in the spherical cell, i.e., $z^* = 1$. Equation 16 holds for monomers that are part of a linear piece. However, for a branching point of a dendrimer not two parts of the molecule come together but more; i.e., $\tau + 1$ branches come together. For a dendrimer that is grafted at one end and the τ branches are chemically the same, eq 16 changes to

$$\varphi_p(z,s) = C_p \frac{G_p(z,s|z^*,1)(G_p(z,s|E))^\tau}{G_p(z)^\tau} \qquad (18)$$

in which segment s is a branch point from which $\tau + 1$ branches depart.

The density distributions of all monomeric components $x \in \{S, Na^+, Cl^-\}$ follow directly from $G_x(z)$, and eq 16 now reduces to $\varphi_x(z) = \varphi_x^b G_x(z)$. Note that $\varphi^b{}_{Na^+} = \varphi^b{}_{Cl^-}$ as the electrostatic potential vanishes in the bulk of the solution.

The set of equations as presented in this section is closed but should be complemented by boundary conditions. As the cell is electroneutral as a whole, we set the "reflecting" boundary conditions at $z = M$, which

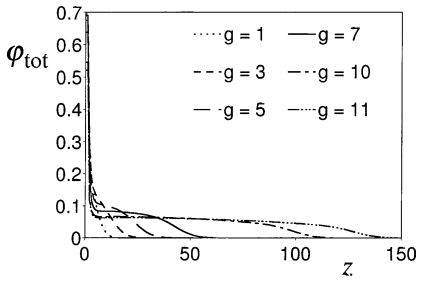

Figure 3. Monomer density profiles for neutral starburst polymers with different number of generations, $g = 1$, 3, 5, 7, 10, and 11, $n = 50$, and Θ-solvent conditions.

guarantees that there are no gradients present in the z direction between $z = M$ and $z = M + 1$: i.e., $\psi(M+1) = \psi(M)$, $u_x(M+1) = u_x(M)$, etc.

The above set of equations are solved iteratively by a Newton-like method. This results in radial distributions of overall monomer densities, P, S, Na^+, Cl^-, as well as, e.g., the densities of end segments and branch points, the segment potentials, and the electrostatic potential. It is also easy to obtain measures for the size of the dendrimer, such as the first moment of the distribution of end segments E:

$$R = \frac{\sum_{z=z^*}^{M} L(z)(z - z^*)\varphi_p(z,E)}{\sum_{z=z^*}^{M} L(z)\varphi_p(z,E)} \qquad (19)$$

Parameters are taken as simple as possible: $\chi_{xy} = 0$ when both x and y are not P, in a good solvent $\chi_{Py} = 0$, and under Θ-conditions $\chi_{Py} = 0.5$. The valences are defined as follows: $\nu_S = 0$, $\nu_{Na^+} = 1$, $\nu_{Cl^-} = -1$, and $\nu_P = -\alpha$. The last statement means that every monomer has the same charge, which is between 0 and −1.

5. Results of the SCF Modeling

5.1. Neutral Starbursts. First, we start with analyzing the overall size of the starburst as a function of the total number of monomer N (or the number of generations g). This will be followed by the discussion on the intrinsic structure of the noncharged starburst.

In Figure 2 the size of a starburst polymer calculated for good and Θ-solvent conditions is presented. We find that in both cases predicted scaling exponents (eq 8) describe the data (at least in the range of g considered) reasonably well.

In Figure 3, the monomer density profiles are presented for a neutral starburst polymer in Θ-solvent for different number of generations g. It is clear from this figure that the monomer density is always a decreasing function of the distance from the center. With increasing number of generations g the density profiles change their shape, and the quasi-plateau region in the density profiles appears.

Remarkably, in the range of g considered here, the average intramolecular density decreases with increasing g. Only for larger number of generations, when inner spacers reach their limit of extension, $g > 10$, the intramolecular density starts to increase (for $g = 11$ this effect is still hardly visible, see Figure 3). The larger is the number of monomers in a spacer, the larger is the number of generations at which the intramolecular density starts to increase.

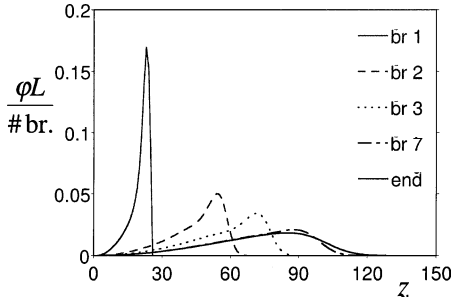

Figure 4. Radial distributions of the branching points and end segments for a neutral starburst polymer with $g = 10$ generations, $n = 50$, and Θ-solvent conditions.

Hence, with increasing g the starburst polymer acquires the density distribution close to that of the uniform sphere. The question remains, how is this flat density profile compatible with the starburst topology, which leads to exponential increase in the number of monomers with increasing ranking number of the generation?

The answer to this question can be found in Figure 4, where we present the radial distribution of the branching points in the neutral starburst polymer with $g = 10$ generations. The figure indicates strong fluctuations of the radial position of the branching points corresponding to all the generations as well as that of the end segments. With increasing ranking number of the branching point the center of the corresponding distribution is displaced toward the periphery and the distribution gets wider, but always ranges down to the center. The distribution of the first branching point is rather strongly peaked almost around the limit of maximal extension (the contour length of a spacer).

This behavior is reminiscent of the quasi-critical fluctuations in a planar polymer brush,[33,34] but very different from what one finds in a starlike polymer. In the latter case the radial distribution of the end segments (and of any internal segments of the branches) is peaked at certain radial distance and exhibits a pronounced dead zone close to the center.[35,36]

The power law radial decay of the monomer density profile inside the star polymer is inherently related to this weak fluctuation of extension of the branches: the self-consistent molecular field strongly pushes the end segments of the branches out from the dense central regions of the star. In contrast to starlike polymers, the intramolecular density in starbursts only weakly decreases as a function of a distance from the center due to increasing number of monomers in outer generations. This situation is reminiscent of that in planar polymer brushes, where the polymer density decreases as a function of the distance from the grafting plane, but weaker than a power law. Therefore, the intramolecular self-consistent potential is not steep enough to induce formation of a dead zone in the central region of a starburst.

The same trends are also observed for a neutral starbursts in good solvent conditions. The results are not shown because the results are qualitatively the same. For the charged starbursts, in all the cases the Θ-solvent conditions with respect to the interactions of uncharged monomers are used.

5.2. Charged Starbursts. The effect of ionization of monomers on the size and internal structure of the starburst polymers is described in this subsection.

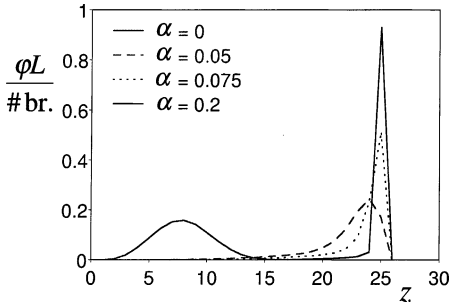

Figure 5. Distribution of the total number of segments of the first branching point of a charge dendrimer with five generations and α as denoted in the graph.

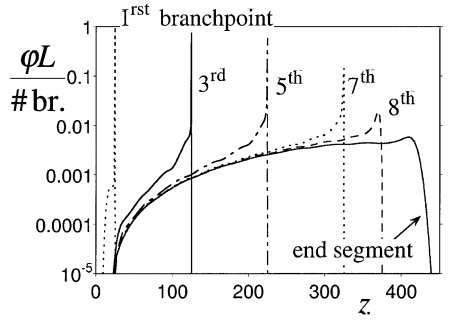

Figure 6. Distribution of the number of the branch points for a dendrimer with $g = 10$ and $\alpha = 0.2$. The distribution is normalized to the total number of those branchpoints in a dendrimer, as denoted by "# br." and given in a semilog scale.

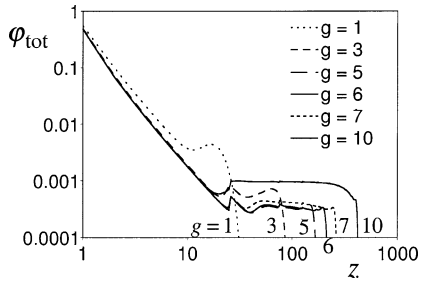

Figure 7. Monomer density profiles of a starburst polymers with $\alpha = 0.2$ for different number of generations, $g = 1$, 3, 5, 6, 7, and 10, $n = 50$, and Θ-solvent conditions.

Figure 5 presents the evolution of the radial distribution of the first branching points with increasing fraction of charged monomers for a starburst of five generations. The maximal stretching of the first branching point is 25. (According to the computation scheme, the center of the cell coincides with the middle monomer of the "root" spacer.) It is well seen in Figure 5 that even weak charging induces so strong pulling out force from the exterior to the central spacers that they get almost completely extended already for $\alpha = 0.1$. Of course, this effect will be even more pronounced for starburst polyelectrolytes with larger number of generations. For example, in Figure 6 we present the radial distributions of the branching points for the starburst of 10 generations with 20% of charged monomers. We see that up to the seventh generation the spacers are fully extended (distributions are almost delta-peaked near limit of extension; the maximal extension is given by $n(g - 1/2)$) while the distribution for a few outer generations and for the end segments are very wide, which ensures fairly constant density inside the dendrimers as seen for charged starbursts in Figure 7 (cf. Figure 3 for noncharged starbursts). These results are also consistent

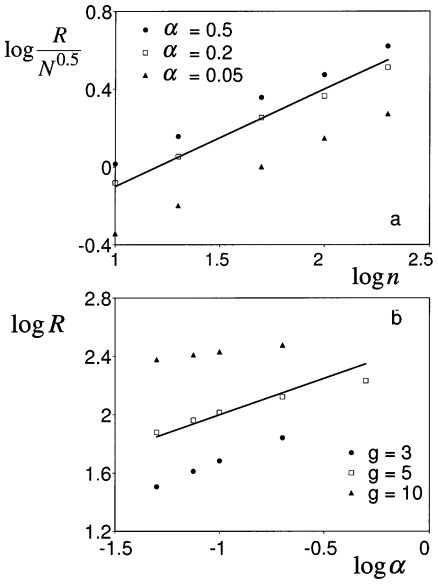

Figure 8. Size of a starburst polyelectrolyte as a function of n or α. (a) The size divided by $N^{1/2}$ as a function of the number of monomers in a spacer n for different α as is denoted in the graph. (b) The size as a function of the degree of charge α, n is 50, and the number of generations g is denoted in the graph. All the graphs are in a log−log scale, and the lines denote the predicted scaling behavior (see eq 10).

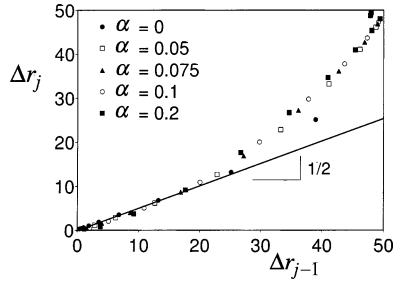

Figure 9. Stretching of a spacer between to branches as a function of the stretching of the spacer from one "generation" lower. The dendrimer has 10 generations, $n = 50$, and α is denoted in the graph. The line with slope $^1/_2$ denotes Gaussian behavior.

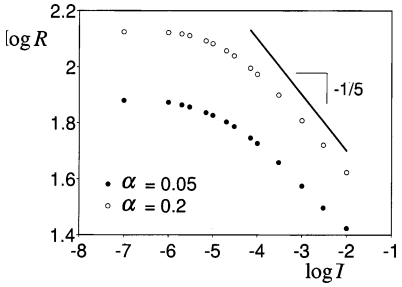

Figure 10. Size of a starburst polyelectrolyte as a function of salt concentration, $n = 50$, α = 0.05, and α = 0.2.

with the relatively broad radial distribution of the position of the end segments observed in Monte Carlo simulations.[12]

In Figure 7, the monomer density profiles for charged dendrimers of different generations are shown. In comparison to Figure 3, an increase in the average density upon an increase in the number of generations is already seen for $g = 7$ generation in stead of $g > 10$ (in the neutral case). Furthermore, a pronounced minimum in the volume fraction profiles is seen at the radial distance corresponding to the average position of the first branching point. This minimum appears also for the noncharged dendrimers for large number of generations, but it is not seen graphically. This minimum was also found in MC simulations.[3,8] The origin of this minimum (and also that of weaker minima close to the average positions of the next branching points) is due to the extensive stretching of the spacer of the inner generations: after the branching points the number of monomers increases by a factor of 2 whereas the volume of the next layer also increases but by a factor that is smaller than 2.

In Figure 8, the calculated size of a starburst as a function of N, n, and α is compared to the power law dependences predicted by eq 10. The scaling exponents for the dependences of the size on the total number of monomers, N, and on the spacer length, n, describe the data quite satisfactory. The slope of the ln R vs ln α dependence progressively decreases with increasing number of generations: for $g = 3$ it is larger that $^1/_2$ (cf. eq 13), for $g = 5$ it is close to the predicted value $^1/_2$, but for $g = 10$ the dependence almost levels off. This behavior at large g is, of course, due to the limit of stretching of spacers of inner generations which is attained for $g = 10$ already at small values of α.

The effect of the salt concentration on the size of the starburst polyelectrolytes is shown in Figure 10. Even for dendrimers with a small fraction of charged monomers, i.e., α = 0.05, the effect of the salt is well pronounced. From the scaling analysis a decrease of the size due to an increase in salt concentration goes with a power law exponent of −1/5. The calculated slope of the decrease is a bit larger; this is due to the high density, i.e., ternary interaction cannot be ignored. However, the slope is fairly good described by the scaling $R \sim c_s^{-1/5}$.

6. Discussion and Conclusions

We have presented a scaling theory of weakly charged starburst polyelectrolytes in salt-free and salt-added solutions. The theory enables us to obtain the power law dependences for the equilibrium dimensions of starburst polyelectrolytes as a function of the number of generations, spacer length, degree of ionization, and the concentration of added electrolyte. The theory is based on the assumption of Gaussian elasticity of spacers.

We have demonstrated that charge renormalization (localization of counterions) occurs for starburst polyions in a salt-free solution similarly to branched polyelectrolytes of other topologies (stars, randomly branched, etc.) when the number of generations exceeds a certain characteristic value. Addition of salt to the solution leads to a decrease in the size due to screening of electrostatic interactions between the branches.

To get more insight into the internal structure of ionic starbursts (that still remains a matter of controversial discussions), we have performed extensive numerical SCF calculations.

The important physical conclusions extracted from the results of these calculations are the following:

i. Whatever the repulsive intramolecular interactions are (short-range excluded volume, long-range Coulomb), the starburst polymer is characterized by a monotonically decreasing density profile in the radial direction. This is in agreement with earlier SCF and MC results for neutral flexible chain dendrimers.

ii. When the number of generation is sufficiently large, the monomer density profile exhibits a quasi-

plateau in the central region of the starburst macromolecule, which is in agreement with experimental observations. This quasi-uniform density distribution is ensured by strong fluctuations in the extensions of the branches, especially those of later generations.

iii. We observe a strong "pulling-out" effect of outer generation onto the spacers of inner generations: with increasing number of generations (i.e., increasing total length of the branches), the stretching of the spacers of inner generations sharply increases. This effect has no analogy for star-branched polymers, polymer brushes, etc., where the structure of the interior regions is not affected by the periphery.

iv. With increasing the total number of generations the spacers belonging to earlier generations get completely extended. This effect is more pronounced for charged starbursts in the salt-free (osmotic) regime. In this case the radial fluctuations of the positions of the corresponding branching points get strongly suppressed.

The main limitation of the presented above analytical theory is due to assumed Gaussian elasticity of spacers. As a result, this theory is quantitatively correct only for starbursts with limited number of generations, long spacers, and weak intramolecular interactions. To describe correctly structure of a starburst with many generations (with strongly extended spacers), one has to take into account finite extensibility (nonlinear elasticity) of spacers together with the fluctuations of the positions of the branching points. The finite extensibility of spacers leads to the limit in the number of generations allowed (space-filling constraint).

The advantage of the our analytical theory, however, is that it enables (i) to predict simple power law dependences for the size of "sparse" starbursts, which cannot be done in a general case within a nonlinear approach, and (ii) to capture some essential features appearing particularly for the charged starbursts whose structural properties are governed by the Coulomb interactions.

In the above-presented theory an equilibrium with respect to ionization/recombination of dissociating monomers with the counterions, e.g., hydrogen ions, is not considered. This effect has to be taken into account for weak (so-called annealed) polyelectrolytes, like poly(acrylic) or poly(methacrylic) acid. The concentration of the hydrogen ions inside the volume occupied by the starburst polyelectrolyte is much higher than in the bulk of the solution. As a result, the ionization of monomers is expected to be strongly suppressed in the starbursts with many generations. We shall consider the charge annealing effect in our forthcoming publication.

Acknowledgment. We are thankful to L. Klushin for helpful discussion and many insightful remarks. This work has been partially supported by the Dutch National Science Foundation (NWO) program "Self-Organization and Structure of Bionanocomposits" No. 047.009.016 and the Russian Foundation for Basic Research (Grant 02-03-33127).

References and Notes

(1) de Gennes, P.-G.; Hervet, H. *J. Phys. (Paris)* **1983**, *44*, L351.
(2) Boris, D.; Rubinstein, M. *Macromolecules* **1996**, *29*, 7251.
(3) Mansfield, M. L.; Klushin, L. I. *Macromolecules* **1993**, *26*, 4262.
(4) Pötschke, D.; Ballauff, M.; Lindner, P.; Fischer, M.; Vöegtle, F. *Macromol. Chem. Phys.* **1999**, *201*, 330.
(5) Pötschke, D.; Ballauff, M.; Lindner, P.; Fischer, M.; Vöegtle, F. *Macromolecules* **1999**, *32*, 4079.
(6) Likos, C. N.; Schmidt, M.; Löwen, H.; Ballauff, M.; Pötschke, D.; Lindner, P. *Macromolecules* **2001**, *34*, 2914.
(7) Likos, C. N.; Rosenfeldt, S.; Dingenonts, N.; Ballauff, M.; Lindner, P.; Werner, N.; Vögtle, F. *J. Chem. Phys.* **2002**, *117*, 1869.
(8) Scherrenberg, R.; Coussens, B.; van Vliet, P.; Eduoard, G.; Brackman, J.; de Brabander, E.; Mortensen, K. *Macromolecules* **1998**, *31*, 456.
(9) Rosenfeldt, S.; Dingenonts, N.; Werner, N.; Ballauff, M.; Vögtle, F.; Lindner, P. *Macromolecules* **2002**, *35*, 8098.
(10) Wind, M.; Saalwachter, K.; Wiesler, U. M.; Mullen, K.; Spiess, H. W. *Macromolecules* **2002**, *35*, 10071.
(11) Murat, M.; Grest, G. *Macromolecules* **1996**, *29*, 1278.
(12) Welch, P.; Muthukumar, M. *Macromolecules* **1998**, *31*, 5892.
(13) Lue, L. *Macromolecules* **2000**, *33*, 2266.
(14) Sheng, Y.-J.; Jiang, S.; Tsao, H.-K. *Macromolecules* **2002**, *35*, 7865.
(15) Giupponi, G.; Buzza, D. M. A. *Macromolecules* **2002**, *35*, 9799.
(16) Mansfield, M. L.; Jeong, M. *Macromolecules* **2002**, *35*, 9794.
(17) Alexander, S.; Chaikin, P. M.; Grant, P.; Morales, G. J.; Pincus, P.; Hone, D. *J. Chem. Phys.* **1984**, *80*, 5776.
(18) Pincus, P. A. *Macromolecules* **1991**, *24*, 2912.
(19) Borisov, O. V. *J. Phys. II* **1996**, *6*, 1.
(20) Borisov, O. V.; Zhulina, E. B. *Eur. Phys. J. B* **1998**, *4*, 205.
(21) Klein Wolterink, J.; Leermakers, F. A. M.; Fleer, G. J.; Koopal, L. K.; Zhulina, E. B.; Borisov, O. V. *Macromolecules* **1999**, *32*, 2365.
(22) Borisov, O. V.; Daoud, M. *Macromolecules* **2001**, *34*, 8286.
(23) Borisov, O. V.; Birshtein, T. M.; Zhulina, E. B. *J. Phys. II* **1991**, *1*, 521.
(24) Zhulina, E. B.; Borisov, O. V. *J. Chem. Phys.* **1997**, *107*, 5952.
(25) Scheutjens, J. M. H. M.; Fleer, G. J. *J. Phys. Chem.* **1979**, *83*, 1619.
(26) Fleer, G. J.; Cohen Stuart, M. A.; Scheutjens, J. M. H. M.; Cosgrove, T.; Vincent, B. *Polymers at Interfaces;* Chapman & Hall: London, UK, 1993.
(27) Israëls, R.; Leermakers, F. A. M.; Fleer, G. J. *Macromolecules* **1994**, *27*, 3087.
(28) van Male, J.; Leermakers, F. A. M.; Fleer, G. J., submitted to *J. Chem. Phys.*
(29) van Male, J.; Leermakers, F. A. M. Computer program "sfbox", 2001.
(30) van Male, J. "Help on sfbox" manuel, Laboratory for Physical Chemistry and Colloid Science, Wageningen University, Wageningen, The Netherlands, 2001.
(31) van der Linden, C. C.; Leermakers, F. A. M.; Fleer, G. J. *Macromolecules* **1996**, *29*, 1000.
(32) Leermakers, F. A. M.; Scheutjens, J. M. H. M. *J. Chem. Phys.* **1988**, *89*, 3264.
(33) Skvortsov, A. M.; Pavlushkov, I. V.; Gorbunov, A. A.; Zhulina, E. B.; Borisov, O. V.; Pryamitsyn, V. A. *Polym. Sci. USSR* **1988**, *30*, 1706.
(34) Klushin, L. I.; Skvortsov, A. M. *Macromolecules* **1991**, *24*, 1549.
(35) Semenov, A. N. *Sov. Phys. JETP* **1985**, *61*, 733.
(36) Grest, G. A.; Kremer, K.; Milner, S.; Witten, T. A. *Macromolecules* **1989**, *22*, 1904.

MA030187P